RSC Advances

RSC Publishing

PAPER

Structure and stability of complexes of charged structural units of heparin with arginine and lysine†

Cite this: *RSC Advances*, 2013, **3**, 1789

Milan Remko,*[ab] Piet Th. Van Duijnen[c] and Ria Broer[c]

Received 5th September 2012,
Accepted 23rd November 2012

DOI: 10.1039/c2ra22062h

www.rsc.org/advances

Our work reports in detail the results of systematic large-scale theoretical investigations of the complexes modeling heparin–protein interaction ($CH_3OSO_3^-\cdots Arg^+$, $CH_3NHSO_3^-\cdots Arg^+$, $CH_3CO_2^-\cdots Arg^+$, $CH_3OSO_3^-\cdots Lys^+$, $CH_3NHSO_3^-\cdots Lys^+$, $CH_3CO_2^-\cdots Lys^+$, $CH_3OPO_3H^{2-}\cdots Arg^+$, $CH_3OPO_3H^{2-}\cdots Lys^+$, $CH_3O(CH_3)PO_2^-\cdots Arg^+$, $CH_3O(CH_3)PO_2^-\cdots Lys^+$, 1,4-DiOMeIdoA2SNa$^-\cdots Arg^+$, 1,4-DiOMeIdoA2SNa$^-\cdots Lys^+$) using Becke3LYP and B97D levels of the density functional theory, as well as at MP2 *ab initio* method. Although initial geometries of complexes paired anionic and cationic species (ionic hydrogen bonds), full geometry optimization of isolated systems resulted in several cases with relaxed geometry and complexes stabilized *via* neutral hydrogen bonds. Hydration caused appreciable geometry changes, especially for substituents (carboxylate and sulphate groups) of the saccharidic part of the complex. The computed Gibbs energies ΔG° of the ionic hydrogen bond systems are negative and high (from −340 to −450 kJ mol^{-1}). In complexes with neutral H-bonds the large destabilizing effect of entropy drives the association reaction to the left. However, owing to a sufficient enthalpy change Gibbs energies are indeed negative, but small (from −20 to 0 kJ mol^{-1}) and the tendency to associate in gas-phase for the complex $CH_3OPO_3H^-\cdots Lys^+$ is negligible. The phosphate anion in its complexes with arginine and lysine proved the lowest tendency to associate. Displacing of Na^+ ions from heparine binding sites by protonated arginine and lysine molecules resulted in positive reaction energies. Solvent (water) reversed the reactivity. Reaction energies computed for the reactions conducted in water are calculated negative, *i.e.* water drives these reactions to the right.

Introduction

Complex saccharides, which are part of the extracellular environment, play important roles in numerous physiological and pathological processes, such as hemostasis, growth factor control, anticoagulation, and cell adhesion.[1–4] An understanding of how these complex saccharides interact with proteins is of great pharmacological interest. Heparin is a heterogeneous polymer constituted of repeating disaccharide sequences of hexuronic acid (D-glucuronic, L-iduronic) and D-glucosamine.[5,6] These residues are substituted with *N*- or *O*-sulfate groups with various degrees of substitution. Heparin and its derivatives are traditional anticoagulants,[5–7] which are used in clinics for the prevention and treatment of thrombosis.[1] Its main antithrombotic activity is explained by its ability to potentiate the activity of serine protease inhibitor antithrombin (AT), which inactivates a number of serine proteases—such as thrombin and factor Xa—in the coagulation cascade.[5,8] High-affinity binding of AT to heparin depends on the presence of a pentasaccharide structural unit containing 3–O sulfates on a heparine residue.[9] It was found that this unique pentasaccharide fragment (PS) constitutes the minimal binding domain for AT. It contains five *O*–sulfate groups, three *N*–sulfate groups and two carboxylate moieties, which are in the isolated molecule coordinated by ten sodium cations. In the antithrombin–pentasaccharide complex, these acidic groups are completely ionized and interact with the complementary (Arg, Lys, Glu and Asn) side chains on the protein.[10–14] The experimental data accumulated over the period of the last 20 years indicate that both arginine and lysine are the most accessible binding sites of proteins in their interaction with anionic sulfate and carboxylate groups of heparin.[15–19] Systematic analyses of the structural crystallographic data of the heparine and its derivatives with proteins have shown that Arg and Lys residues of proteins are clearly in the position to have hydrogen bond interaction with the negatively charged sulfate and carboxylate groups of heparin pentasaccharide.[4,20–24] The bulk of these hydrogen bonds are sulfate-mediated interactions (consequently without exact data on the positions of hydrogen atoms). However, despite their great pharmaco-

[a]*Department of Pharmaceutical Chemistry, Comenius University in Bratislava, Odbojarov 10, 832 32, Bratislava, Slovakia*
[b]*Center for Hemostasis and Thrombosis, Hemo Medika Bratislava, 851 04, Bratislava, Slovakia*
[c]*Department of Theoretical Chemistry, Zernike Institute for Advanced Materials, University of Groningen, Nijenborgh 4, 9747 AG, Groningen, The Netherlands*
† Electronic supplementary information (ESI) available. See DOI: 10.1039/c2ra22062h

logical importance, the detailed nature of these interactions remains one of the structurally and energetically less well characterized.

The present paper reports in detail the structural parameters of the Arg and Lys interaction with the sulfate and carboxylate interaction sites of glycosaminoglycans. They are chosen to model the characteristic interaction of heparin with proteins (Fig. 1). Various levels of *ab initio* self-consistent field (SCF) and density functional (DFT) were applied for this investigation. The effect of water and the effect of displacement of heparin-bound counterions on the nature of this interaction were also investigated. The results of these model studies are discussed and compared with the available experimental results for structurally related systems and discussed with the present theories of action of these glycosaminogycans.

Computational details

The geometries of all molecular complexes investigated ($CH_3OSO_3^-\cdots Arg^+$, $CH_3NHSO_3^-\cdots Arg^+$, $CH_3CO_2^-\cdots Arg^+$, $CH_3OSO_3^-\cdots Lys^+$, $CH_3NHSO_3^-\cdots Lys^+$, $CH_3CO_2^-\cdots Lys^+$, $CH_3OPO_3H^{2-}\cdots Arg^+$, $CH_3OPO_3H^{2-}\cdots Lys^+$, $CH_3O(CH_3)PO_2^-\cdots Arg^+$, $CH_3O(CH_3)PO_2^-\cdots Lys^+$, 1,4-DiOMeIdoA2SNa$^-\cdots Arg^+$, 1,4-DiOMeIdoA2SNa$^-\cdots Lys^+$) have been completely optimized with the Gaussian 03 and Gaussian 09 programs,[25,26] using density functional theory[27–29] with the B3LYP hybrid functional[30–32] and B97D Grimme's functional including dispersion,[33] and also with second-order Møller–Plesset perturbation theory (MP2) level using 6-31+G(d,p) basis set as implemented in the Gaussian packages of computer codes.[25,26] The 6-31+G(d,p) basis set was chosen both because of its computational efficiency and for its proven ability to provide optimized structures of ionic hydrogen bonded complexes in a similar manner as basis set of the triple-ζ quality (6-311++G(d,p).[34–36] The interaction energy, ΔE, for the interaction of acid groups of heparine models (H) with Lewis bases (LB) L-lysine and L-arginine is given by the following equation

$$\Delta E = E[\mathrm{H}\cdots\mathrm{LB}] - \{E[\mathrm{H}] + E[\mathrm{LB}]\} \quad (1)$$

where E[H] and E[LB] are the energies of the heparine model acidic groups and Lewis base molecules, respectively, and E[H···LB] is the energy of the complex. Ionic hydrogen bonded complexes are dominated by the electrostatic interactions and thus are reasonably well described by density functional theory (DFT) or MP2.[36,37] Basis set superposition error (BSSE) was corrected following Boys and Bernardi.[38] In order to evaluate the effect of different computational methods on the computed parameters, interaction energies and geometries of ionic complexes are evaluated at both MP2 (frozen core, FC) and DFT levels of theory. The majority of the calculations were carried out using density functional theory with the B3LYP and B97D functionals. Thermodynamic functions for all complexes studied were computed at the B3LYP/6-31+G(d,p) level of model chemistry. Interaction energies of ionic complexes computed using the double-ζ 6-31+G(d,p) basis set are always, by about 5-10 kJ mol^{-1}, higher than those of the more accurate[39,40] calculations using the triple-ζ basis set. However, the relative trends in the individual stability of ionic complexes are equally reproduced by both methods. Thus, the B3LYP/6-31+G(d,p) method should be used as a relatively inexpensive alternative for the study of the coordination of oligomeric structural units of heparin with Lys and Arg structural units of proteins. Solvent effects on the species studied were evaluated using the polarizable conductor calculation model (CPCM).[41–44] The structures of all gas-phase and condensed-phase (CPCM) species were fully optimized without any geometrical constraint.

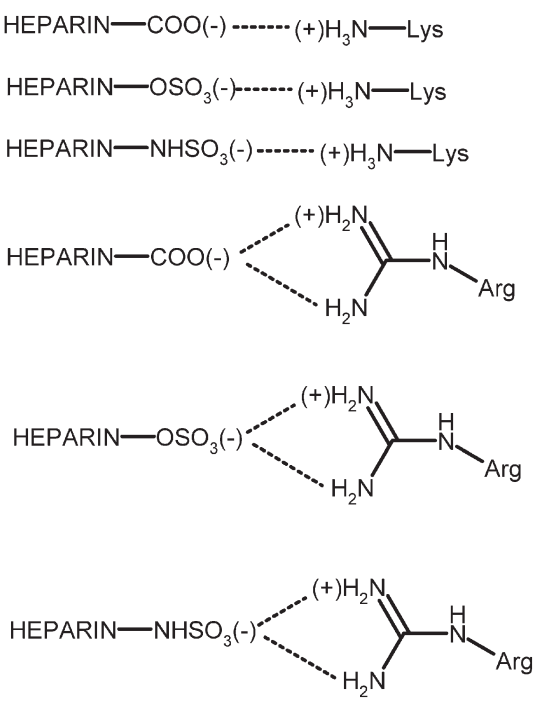

Fig. 1 Schematic representation of charged heparine–amino acid interactions.

Results and discussion

General considerations

Heparin, its low molecular weight derivatives and synthetic pentasaccharides exert their anticoagulant activity through the binding and activation of antithrombin III (ATIII, a coagulation protease inhibitor).[8,10] An understanding of the subtle details of these interactions is of great therapeutic importance. Experimental structural investigations using NMR spectroscopy or X-ray analysis of the complexes of heparine and its derivatives with suitable proteins brought some insight into the origin of these interactions.[8,24]

With the aim of more obtaining detailed specification of the origin of the interaction of anionic sulfate and carboxylate groups of gycosaminoglycan (GAG) with proteins we applied the program GlyVicinity.[45–48] This software enables an analysis

of amino acids in the vicinity of carbohydrate residues contained in the Protein Data Bank (PDB). For an analysis of GAG – protein interactions, three X-ray complexes of pentasaccharide with ATIII contained in the PDB (1AZX, 1E03 and 1NQ9, respectively) were chosen. It was found that of a total of 129 amino acids analyzed in the vicinity of 30 carbohydrate residues, 67 interactions or 52% of contacts with the pentasaccharide carboxylate and sulfate groups belong to the Arg and Lys of ATIII. Based on these results and the experimental evidence of the importance of GAG-protein interaction for drug design and development[10,19,20,23,24] we used *ab initio* molecular orbital methods to study the interactions between models of heparine negatively charged sulfate and carboxylate structural units and complementary positive charged arginine and lysine structural units of ATIII. The sulfated and acetylated groups of heparin were modelled by acetylate, methylsulfate and methylsulfamic acid anions, respectively. A sugar moiety of GAG was represented by the energetically stable skew-boat ^2S_o conformer[40,49,50] of the substituted iduronic acid derivative 1,4-DiOMeIdoA2S (unit G of the pentasaccharide). Amino acids arginine and lysine emulated the appropriate portions of the receptor (ATIII). Anions of the monomethyl ester of methylphosphonic acid and the methyl ester of phosphoric acid represent bioisosteric substitution of the sulphate group in native GAG. The input geometries of all molecules investigated were constructed using the molecular modelling tool and the definition of approximate values of the conformational parameters for the pyranose ring of the skew-boat conformer of 1,4-DiOMe IdoA2S (in the form of its sodium salt 1,4-DiOMeIdoA2SNa$_2$).[40,49,50] As an illustration of the overall shape of the fourteen complexes investigated in Fig. A of the ESI† molecular structures and geometries of the complexes studied, computed at the Becke3LYP/6-31+G(d,p) level of theory, are presented. An analysis of the harmonic vibrational frequencies of the optimized species computed at the Becke3LYP level of theory also proved that all of them are minima (zero number of imaginary frequencies). The monomeric structures considered in our calculations represent strong acids and/or bases (Table 1) which, at physiological pH = 7.4, are completely ionized and/or protonized. Although the initial geometries of complexes of paired anionic and cationic species (ionic hydrogen bonds), full geometry optimization of the systems resulted in several cases with relaxed geometry and comple stabilized *via* neutral hydrogen bonds. In order to check the possible proton transfer converting a stable ion pair complex to a neutral H-bond we also optimized geometry of neutral H-bonded complexes. However, the second energy minimum was not observed and/or it was a local minimum (complexes **4** and **11**). The geometric parameters associated with intermolecular $O^-\cdots H\text{–}N^+$ or $O\text{–}H\cdots N$ interactions are listed in Table 2. The length of these hydrogen bonds ranges from 2.589 to 3.119 Å. Regarding protonated arginine, pairing with the negatively charged sulphate and carboxylate groups resulted in the ionized H-bonded complexes (systems **1–3**, **11**, **12**, Table 2). These complexes are stabilized by two almost symmetrical ionic linear hydrogen bonds of the $O^-\cdots H\text{–}N^+$ type. The situation with the interaction of protonated lysine molecule is different. In the complexes involving the *O*-sulphate group (complexes **4** and **14**, Table 2) the NH_3^+ moiety is coordinated *via* two unsymmetrical $O^-\cdots H\text{–}N^+$ H-bonds to two oxygen atoms forming bent hydrogen bonds with the $O^-\cdots H\text{–}N^+$ angles of about 130°–155°, respectively. During optimization of the charged lysine complexes containing *N*-sulphate and carboxylate groups, respectively, proton transfer has been observed. The optimal conformation is stabilized by means of one linear $O\text{–}H\cdots N$ hydrogen bond (systems **5**, **6** and **13**, Table 2). Complexes **7–10** model the interaction of structurally modified GAG with Arg or Lys in which an *O*-sulphate group of the native derivative is replaced by phosphate and/or methyl-phosphonate moieties. Optimization at both DFT and MP2 levels of theory of complexes **7**, **8** and **10** resulted in relaxed species stabilized by neutral H-bonds of the $P{=}O\cdots H\text{–}N$ type. However, the dianion of the methyl ester of phosphoric acid is not able to attract any proton from the guanidinium group of Arg, and this complex is stabilized *via* two ionic H-bonds (system **9**, Table 2). Equilibrium hydrogen bond geometries computed at the DFT level are close to these obtained using MP2 theory. In general, the MP2 hydrogen bonded distances are always longer by about 0.05 Å. As an example, the structure of the $CH_3OSO_3^-\cdots Arg^+$ complex computed at both levels of theory is presented in Fig. 2. The hydrogen bond moieties discussed and the molecular structure of the complexes studied, are based on calculations *in vacuo*. Because the complex GAG–protein interactions in reality takes place in water, we also examined the solvent effects. The effect of bulk solvent is treated with the CPCM solvation method. The polarizable continuum model (CPCM) defines the cavity as the union of a series of interlocking atomic spheres.[42–44] Continuum-based methods of solvation are used extensively and successfully in a variety of problems including drug molecules.[54,55] Water has a remarkable effect especially on the geometry of the structurally flexible polar parts of the systems studied. The changing of the molecular structure of the solvated complex is illustrated on the 1,4-DiOMeIdoA2SNa$^-\cdots Arg^+$ complex **12**, Fig. 3. Hydration caused appreciable geometry changes, especially for substituents (carboxylate and sulphate groups) of the saccharidic part of the complex. In Table 3 water stabilization energies are listed for CPCM fully optimized geometries. All three levels of theory applied suggest that the solvation energy is large and stabilizing. Because of the negative charge (−1) of complexes **7** and **8**, containing a phosphate group, is energetically the most

Table 1 pK_a values of the studied compounds

Acid (Base)	pK_a (H_2O)
CH_3COOH	4.76[a]
CH_3OSO_3H	0.42[b]
CH_3NHSO_3H	1.73[b]
1,4-DiOMeIdoA2S	0.25[b] (–OSO_3H); 3.67[b] (–COOH)
$CH_3OPO_3H_2$	1.11[b] (O^-); 6.38[b] (O^{2-})
$CH_3O(CH3)PO_2H$	2.31[b]
Arginine	12.48[a] (side chain)
Lysine	10.53[a] (side chain)

[a] Experimental values of pK_a were taken from pK_a data compiled by R. Williams, ref. 51. [b] Computed data using software Sparc.[52,53]

Table 2 Hydrogen bonds geometry (Becke3LYP method)

No.	System	Hydrogen bond type	N–H	*O*–H	O···N	O···H···N
1	$CH_3OSO_3^-\cdots Arg^+$	$O^-\cdots H–N^+$	1.049; 1.053[a]		2.688; 2.682	175.1; 178.7
2	$CH_3NHSO_3^-\cdots Arg^+$	$O^-\cdots H–N^+$	1.054; 1.056[a]		2.676; 2.672	177.1; 178.9
3	$CH_3CO_2^-\cdots Arg^+$	$O^-\cdots H–N^+$	1.101; 1.078[a]		2.580; 2.629	179.7; 178.2
4	$CH_3OSO_3^-\cdots Lys^+$	$O^-\cdots H–N^+$	1.079; 1.043[a]		2.605; 2.698	155.7; 137.2
5	$CH_3NHSO_3^-\cdots Lys^+$	*O*–H···N		1.076	2.578	175.5
6	$CH_3CO_2^-\cdots Lys^+$	*O*–H···N		1.019	2.706	170.4
7	$CH_3OPO_3H^{2-}\cdots Arg^+$	*O*–H···N	1.055	0.988	2.886[b]; 2.706[c]	178.2[b]; 174.9[c]
8	$CH_3OPO_3H^{2-}\cdots Lys^+$	*O*–H···N	1.034	0.978	3.034[b]; 2.858[c]	155.5[b]; 157.1[c]
9	$CH_3O(CH_3)PO_2^-\cdots Arg^+$	$O^-\cdots H–N^+$	1.077; 1.075[a]		2.617; 2.620	178.8; 179.4
10	$CH_3O(CH_3)PO_2^-\cdots Lys^+$	*O*–H···N	1.023	1.028	2.662[b]; 3.119[c]	166.6[b]; 128.1[c]
11	1,4-DiOMeIdoA2SNa(COO^-)···Arg^+	$O^-\cdots H–N^+$	1.074; 1.077[a]		2.635; 2.628	178.4; 178.2
12	1,4-DiOMeIdoA2SNa(OSO_3^-)···Arg^+	$O^-\cdots H–N^+$	1.046; 1.050[a]		2.708; 2.688	176.4; 179.1
13	1,4-DiOMeIdoA2SNa(COO^-)···Lys^+	$O^-\cdots H–N^+$		1.025	2.679	171.9
14	1,4-DiOMeIdoA2SNa(OSO_3^-)···Lys^+	*O*–H···N	1.085; 1.037[a]		2.589; 2.725	158.6; 131.9

[a] Two H-bonds. [b] O–H···N H-bond. [c] N–H···O H-bond.

feasible process in water. The CH_3CO_2···Lys complex **6** is in aqueous solution stabilized at least by about −50 kJ mol^{-1}. The geometry optimization in water of the complexes **4**, **5** and **10** pairing the lysine cation with carboxylate, *N*-sulphate and methyl phosphonate anions reversed the stability of these systems. In contrast with the gas-phase, in solution these complexes exist in a more stable charged complex of the $O^-\cdots H–N^+$ type (Table 3). In general, solvation results in an appreciable stabilization of complexes in the solvated state (Table 3).

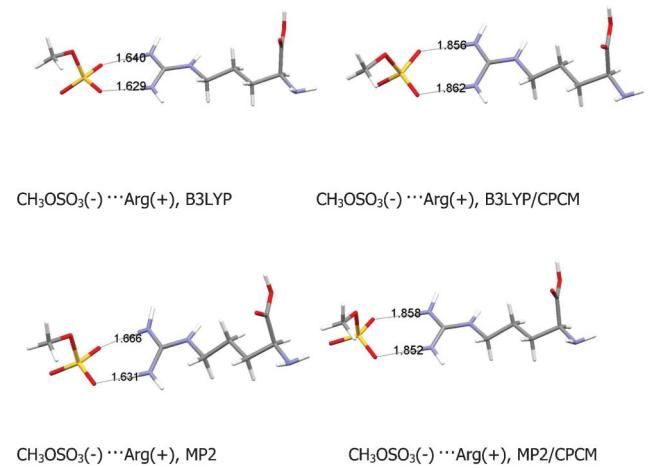

Fig. 2 Solvent effect on the geometry of $CH_3OSO_3^-\cdots Arg^+$ complex computed using two methods of model chemistry.

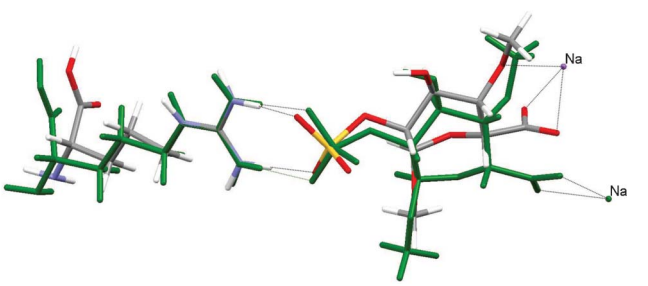

Fig. 3 Molecular superimposition of the 1,4-DiOMeIdoA2SNa···Arg complex and in solution optimized 1,4-DiOMe IdoA2SNa···Arg system (green).

Energy of hydrogen-bonded complexes

The interaction energies of the complexes studied computed at the B3LYP, B97D levels of density functional theory and MP2(FC) level of *ab initio* SCF method are given in Table 4. The correction of the hydrogen bond energy for the superposition error (BSSE) determined at the potential minimum does not alter the relative stability order of the complexes investigated. The Grimme's B97D uses the empirical dispersion energy correction specifically designed for accurate evaluation of van der Waals complexes.[33] The Δ*E*s at this level are 5–40 kJ mol^{-1} more negative than with B3LYP, and the relative stabilities of individual hydrogen bonded complexes are by both DFT methods described equally. H-bonding complexes investigated are dominated by the electrostatic interactions and the dispersion, otherwise present in this interaction, does not

Table 3 Computed solvent stabilization energies ΔE^{CPCM} (kJ mol^{-1}) of the complexes studied in water solution (T = 298.15 K)

No.	System	ΔE^{CPCM}		
		B3LYP	B97D	MP2
1	$CH_3OSO_3^-\cdots Arg^+$	−128.22[a]	−122.89[a]	−128.68[a]
2	$CH_3NHSO_3^-\cdots Arg^+$	−130.26[a]	−124.67[a]	−131.37[a]
3	$CH_3CO_2^-\cdots Arg^+$	−95.65[a]	−89.78[a]	−82.26[a]
4	$CH_3OSO_3^-\cdots Lys^+$	−116.68[a]	−110.68[a]	−117.65[a]
5	$CH_3NHSO_3^-\cdots Lys^+$	−123.67[a]	−110.86[a]	−128.14[a]
6	$CH_3CO_2^-\cdots Lys^+$	−49.50[b]	−53.05[b]	−49.66[b]
7	$CH_3OPO_3H^{2-}\cdots Arg^+$	−321.94[b]	−315.21[b]	−317.21[b]
8	$CH_3OPO_3H^{2-}\cdots Lys^+$	−292.04[b]	−286.04[b]	−288.98[b]
9	$CH_3O(CH_3)PO_2^-\cdots Arg^+$	−108.69[a]	−104.17[a]	−110.09[a]
10	$CH_3O(CH_3)PO_2^-\cdots Lys^+$	−80.10[a]	−76.01[a]	−88.13[a]
11	1,4-DiOMeIdoA2SNa(COO^-)···Arg^+	−241.34[a]	−245.11[a]	
12	1,4-DiOMeIdoA2SNa(OSO_3^-)···Arg^+	−283.01[a]	−262.67[a]	
13	1,4-DiOMeIdoA2SNa(COO^-)···Lys^+	−203.19[b]	−211.71[b]	
14	1,4-DiOMeIdoA2SNa(OSO_3^-)···Lys^+	−274.83[a]	−264.87[a]	

[a] Ionic hydrogen bond. [b] Neutral hydrogen bond.

Table 4 Computed interaction energies ΔE (kJ mol^{-1}) of the hydrogen bonded complexes studied (T = 298.15 K)

No.	System	ΔE, MP2	ΔE, B3LYP	ΔE, B97D
1	$CH_3OSO_3^-\cdots Arg^+$	−424.47[a]	−428.14[a]	−433.44[a]
2	$CH_3NHSO_3^-\cdots Arg^+$	−437.42[a]	−441.64[a]	−450.23[a]
3	$CH_3CO_2^-\cdots Arg^+$	−75.89[b]	−532.22[a]	−551.67[a]
4	$CH_3OSO_3^-\cdots Lys^+$	−471.95[a]	−477.23[a]	−495.51[a]
5	$CH_3NHSO_3^-\cdots Lys^+$	−98.83[b]	−91.43[b]	−113.58[b]
6	$CH_3CO_2^-\cdots Lys^+$	−70.14[b]	−54.32[b]	−67.65[b]
7	$CH_3OPO_3H^{2-}\cdots Arg^+$	−59.54[b]	−67.23[b]	−76.29[b]
8	$CH_3OPO_3H^{2-}\cdots Lys^+$	−49.25[b]	−47.85[b]	−59.78[b]
9	$CH_3O(CH_3)PO_2^-\cdots Arg^+$	−494.59[a]	−501.83[a]	−509.84[a]
10	$CH_3O(CH_3)PO_2^-\cdots Lys^+$	−64.61[b]	−64.53[b]	−86.82[b]
11	1,4-DiOMeIdoA2SNa(COO^-)$\cdots Arg^+$		−476.53[a]	−488.04[a]
12	1,4-DiOMeIdoA2SNa(OSO_3^-)$\cdots Arg^+$		−405.12[a]	−446.52[a]
13	1,4-DiOMeIdoA2SNa(COO^-)$\cdots Lys^+$		−58.59[b]	−73.29[b]
14	1,4-DiOMeIdoA2SNa(OSO_3^-)$\cdots Lys^+$		−462.89[a]	−490.83[a]

[a] Ionic hydrogen bond. [b] Neutral hydrogen bond.

play any important part in the final stabilization of the hydrogen-bonded complex. The correlate model MP2/6-31+G(d,p), recommended by Del Bene for neutral and ionic hydrogen bonded complexes,[56] describes the stability of all but one complex with the same pattern (Table 4). In the contrast to the DFT, during the MP2 optimization of the $CH_3CO_2^-\cdots Arg^+$ complex, starting from a charged initial geometry, proton transfer has been observed.

Gas phase thermochemistry of hydrogen-bonded complexes

Table 5 summarizes the thermodynamic quantities calculated using the BLYP method for the gas-phase reaction (1). In real molecular complexes, the tendency to associate is described by Gibbs energies. It is, therefore, important to know the role of entropy in the processes studied. Table 5 also lists the differences in S^0 values of the complexes and the isolated species. The formation of a hydrogen-bonded complex from a pair of species necessarily involves a loss of entropy. The entropy change due to complexation is about −130 to −150 J K^{-1} mol and calculated enthalpies and Gibbs energies follow the same tendency in the stability of hydrogen-bonded complexes. The computed Gibbs energies ΔG° of the ionic hydrogen bond systems **1–4**, **9**, **11**, and **12** are negative and high (from −340 to −450 kJ mol^{-1}). In complexes **5–8**, **10**, **13** (neutral H-bonds) the large destabilizing effect of entropy drives the association reaction to the left. However, owing to a sufficient enthalpy change Gibbs energies are indeed negative, but small (from −20 to 0 kJ mol^{-1}) and the tendency to associate in the gas-phase for the complex $CH_3OPO_3H^-\cdots Lys^+$ is negligible (Table 5). The phosphate anion in its complexes with arginine (**7**) and lysine (**8**) showed the lowest tendency to associate (Table 5). It is well known that drug affinity is related not only to structural behavior (enthalpy) but also to the dynamics (entropy) of the interacting species. Hydrogen bonds play an important part in drug–receptor interactions. They are responsible for the directionality of such interaction and they are also important for modification of the affinity of a drug molecule to its receptor.[57,58] The computed (weak) hydrogen bond interaction of the phosphate with cationic lead groups of arginine and lysine (Table 5) correlates very well with the experimentally known fact that replacement of the *O*-sulphate group of pentasaccharide by phosphate led to a complete loss of its biological activity.[59]

Displacement reactions

The interaction of polyanionic glycosaminoglycans with binding proteins is frequently interpreted on the basis of polyelectrolyte theory. According to this theory[17] heparin

Table 5 Becke3LYP gas-phase thermochemistry of the complexation (T = 298.15 K)

No.	System	ΔH, kJ mol^{-1}	ΔS, J K^{-1} mol	ΔG, kJ mol^{-1}
1	$CH_3OSO_3^-\cdots Arg^+$	−404.34	−149.11	−359.91
2	$CH_3NHSO_3^-\cdots Arg^+$	−417.48	−151.96	−372.19
3	$CH_3CO_2^-\cdots Arg^+$	−492.89	−154.56	−446.83
4	$CH_3OSO_3^-\cdots Lys^+$	−445.67	−139.94	−403.97
5	$CH_3NHSO_3^-\cdots Lys^+$	−65.08	−148.11	−20.94
6	$CH_3CO_2^-\cdots Lys^+$	−44.32	−130.85	−5.31
7	$CH_3OPO_3H^{2-}\cdots Arg^+$	−53.13	−149.59	−8.55
8	$CH_3OPO_3H^{2-}\cdots Lys^+$	−41.96	−140.80	0.0
9	$CH_3O(CH_3)PO_2^-\cdots Arg^+$	−466.21	−163.09	−417.59
10	$CH_3O(CH_3)PO_2^-\cdots Lys^+$	−52.02	−151.71	−6.81
11	1,4-DiOMeIdoA2SNa(COO^-)$\cdots Arg^+$	−427.26	−148.41	−383.03
12	1,4-DiOMeIdoA2SNa(OSO_3^-)$\cdots Arg^+$	−378.93	−140.04	−337.19
13	1,4-DiOMeIdoA2SNa(COO^-)$\cdots Lys^+$	−50.46	−138.99	−9.04
14	1,4-DiOMeIdoA2SNa(OSO_3^-)$\cdots Lys^+$	−430.39	−168.18	−380.28

binding to proteins is largely driven by the favourable increase of entropy resulting from the release of ions such as Na^+ from heparin binding sites. It is assumed that also components of Gibbs energy due to hydrogen bonds and hydrophobic interactions are also present.[17] In order to gain more quantitative information about the role of small metal cation coordination at carboxylate and sulphate groups of heparin on the heparin–protein interaction we also modelled the displacement of Na^+ ions from heparine binding sites by protonated arginine and lysine molecules, respectively. The calculated reaction energies, enthalpies, entropies, and Gibbs energies are reported in Table 6. The reaction energies were evaluated as the differences between the total energies of reaction products and reactants. In these calculations, the total energies of the optimized coordinated species were considered. The 1,4-DiOMeIdoA2SNa_2 molecules model sodiated heparine. Reaction energies, ΔE, computed at both levels of theory are high and positive, indicating that the displacement of one sodium cation from its binding site modelled by sodium salts of acids studied (CH_3OSO_3Na, CH_3NHSO_3Na, CH_3CO_2Na, as well as the more complex 1,4-DiOMeIdoA2SNa_2 molecule) is highly endothermic. In general, displacement of a Na^+ cation with charged lysine is less endothermic (reactions **4–6**, **13** and **14**, Table 6). The reaction entropy evaluated at the B3LYP level is negative, *i.e.* destabilizing and results in high positive Gibbs energies of about 55–180 kJ mol^{-1}. However, the computed gas phase sodium affinities of CH_3OSO_3Na, CH_3NHSO_3Na, CH_3CO_2Na, and 1,4-DiOMeIdoA2SNa_2 are negative, and sufficiently stable[60] (from −550 to −650 kJ mol^{-1}) to be displaced by less basic amino acids Arg and Lys cations. Thus gas phase thermochemistry of displacing a sodium ion from its GAG binding site is a highly endothermic process. In reality displacing of sodium ions takes place in aqueous solution. It is therefore instructive to study solvent effects on these reactions. Table 6 also contains reaction Gibbs energies ΔG^{CPCM} for the 10 reactions studied in aqueous solution. To evaluate the effect of the solvent at the B3LYP, B97D and MP2 levels of theory using the conductor like screening model (CPCM) we tested in the calculation of Gibbs energies of hydration of a Na^+ cation for which experimental data are available.[61] The MP2 (−418.17 kJ mol^{-1}) and B97D (−418.29 kJ mol^{-1}) calculations reproduce the experimental standard hydration Gibbs energy of Na^+ (ΔG^{298} = −430. 64 kJ mol^{-1}). By the B3LYP method computed hydration Gibbs energy (−460.42 kJ mol^{-1}) is about 30 kJ mol^{-1} larger. Solvation has a dramatic effect on these reactions. Immersing reactants and reaction products in water produces different solvent stabilization compared to the gas state. Reaction energies computed for the reactions conducted in water are calculated negative, *i.e.* water drives these reactions to the right (Table 6). The ΔEs^{CPCM} at the BLYP level are in most cases 20–40 kJ mol^{-1} more negative than with MP2 in no particular pattern. The lowest negative ΔE^{CPCM} energies are obtained with the B97D method (Table 6). The only exceptions occur with the reaction of CH_3COONa with Arg^+ and Lys^+, respectively. The very high B97D ΔE^{CPCM} of about −160 kJ mol^{-1}, is associated with proton transfer during the optimization procedure of reaction products CH_3CO_2Arg and CH_3CO_2Lys, starting from an ionic H-bond initial geometry. The reason for such a strong solvent effect is a larger stabilization of these species by water.

Clinically useful heparins contain carboxylate and sulphate groups in the neutral state coordinated by sodium cations. During the binding process sodium ions are displaced by complementary charged groups of the side chains of the amino acids of a protein. The polyanionic form of heparin is bound to the protein and thus represents the active species.[8] Our calculations show that the displacement process in aqueous solution is an exothermic reaction and is connected with the formation of strong hydrogen-bonded complexes.

Summary and conclusions

This theoretical study set out to determine geometries and interaction energies of $CH_3OSO_3^-\cdots Arg^+$, $CH_3NHSO_3^-\cdots Arg^+$, $CH_3CO_2^-\cdots Arg^+$, $CH_3OSO_3^-\cdots Lys^+$, $CH_3NHSO_3^-\cdots Lys^+$, $CH_3CO_2^-\cdots Lys^+$, $CH_3OPO_3H^{2-}\cdots Arg^+$, $CH_3OPO_3H^{2-}\cdots Lys^+$, $CH_3O(CH_3)PO_2^-\cdots Arg^+$, $CH_3O(CH_3)PO_2^-\cdots Lys^+$, 1,4-DiOMeIdoA2S$Na^-\cdots Arg^+$, and 1,4-DiOMeIdoA2S$Na^-\cdots Lys^+$ complexes. For these hydrogen-bonded complexes, experimental structural and thermochemical data that consider their

Table 6 Computed reaction energies (kJ mol^{-1}), enthalpies (kJ mol^{-1}), entropies (J K^{-1} mol), Gibbs energies (kJ mol^{-1}) and solvent stabilization energies ΔE^{CPCM} (kJ mol^{-1}) of the ion displacement reactions studied (T = 298.15 K)

No.	Reaction	ΔE		ΔH	ΔS	ΔG	ΔE^{CPCM}		
		MP2	B97D	B3LYP	B3LYP	B3LYP	MP2	B97D	B3LYP
1	$CH_3OSO_3Na + Arg^+ \rightarrow CH_3OSO_3Arg + Na^+$	95.9	111.2	120.8	120.9	−38.1	132.3	−22.5	−11.2	−59.6
2	$CH_3NHSO_3Na + Arg^+ \rightarrow CH_3NHSO_3Arg + Na^+$	106.9	119.9	131.6	131.5	−42.6	144.1	−47.7	−15.4	−61.2
3	$CH_3CO_2Na + Arg^+ \rightarrow CH_3CO_2Arg + Na^+$	86.9	107.5	123.3	118.8	−44.7	132.1	−24.5	−161.1[a]	−66.0
4	$CH_3OSO_3Na + Lys^+ \rightarrow CH_3OSO_3Lys + Na^+$	53.6	67.2	80.3	79.6	−29.0	88.3	−29.5	−7.4	−52.2
5	$CH_3NHSO_3Na + Lys^+ \rightarrow CH_3NHSO_3Lys + Na^+$	72.3	74.6	95.0	89.6	−27.3	97.7	−54.8	−11.3	−54.6
6	$CH_3CO_2Na + Lys^+ \rightarrow CH_3CO_2Lys + Na^+$	29.1	37.1	49.4	47.6	−24.9	55.1	−25.4	−159.2[a]	−57.1
7	1,4-DiOMeIdoA2SNa_2 + $Arg^+ \rightarrow$ 1,4-DiOMeIdoA2SNa(COO^-)$Arg^+ + Na^+$		110.3	124.3	121.7	−51.9	137.2		−20.7	−65.3
8	1,4-DiOMeIdoA2SNa_2 + $Arg^+ \rightarrow$ 1,4-DiOMeIdoA2SNa(OSO_3^-)$Arg^+ + Na^+$		139.7	174.5	175.0	−20.1	181.1		−8.9	−56.8
9	1,4-DiOMeIdoA2SNa_2 + $Lys^+ \rightarrow$ 1,4-DiOMeIdoA2SNa(COO^-)$Lys^+ + Na^+$		46.2	58.8	56.8	−29.7	65.6		−15.9	−56.8
10	1,4-DiOMeIdoA2SNa_2 + $Lys^+ \rightarrow$ 1,4-DiOMeIdoA2SNa(OSO_3^-)$Lys^+ + Na^+$		115.3	125.6	123.6	−48.6	138.1		−13.9	−50.6

[a] Relaxed structure with neutral hydrogen bond.

chemical and biological importance are scarce. The following conclusions can be drawn.

1. Pairing of protonated arginine with negatively charged sulphate and carboxylate groups resulted in the ionized H-bonded complexes **1–3**, **11**, **12**. These complexes are stabilized by two almost symmetrically charged, linear hydrogen bonds of the $O^{-}\cdots H\text{–}N^{+}$ type. A protonated lysine molecule in the complexes involving an *O*-sulphate moiety is coordinated *via* two unsymmetrical $O^{-}\cdots H\text{–}N^{+}$ H-bonds. As regards the charged lysine complexes containing *N*-sulphate and carboxylate groups, respectively, proton transfer has been observed. The optimal conformation is stabilized by a linear O–H···N hydrogen bond (systems **5**, **6** and **13**).

2. Replacement of the *O*-sulphate group by phosphate and/or methyl-phosphonate moieties resulted in relaxed species, stabilized by neutral H-bonds of the P=O···H–N type (complexes **7**, **8** and **10**).

3. Equilibrium hydrogen bond geometries computed at the DFT level are close to these obtained using MP2 theory. In general, the MP2 hydrogen bonded distances are always by about 0.05 Å longer.

4. The calculated solvation energy using CPCM fully optimized geometries is large and stabilizing. Because of the negative charge (−1) of complexes **7** and **8**, containing a phosphate group, is energetically the most feasible process in water. The geometry optimization in water of the complexes **4**, **5** and **10**, pairing lysine cation with carboxylate, N-sulphate and methyl phosphonate anions, reversed the stability of these systems. In contrast with the gas-phase, in solution these complexes exist in a more stable charged complex of the $O^{-}\cdots H\text{–}N^{+}$ type.

5. Displacing of Na^{+} ions from heparine binding sites by protonated arginine and lysine molecules resulted in positive reaction energies. Solvent (water) reversed the reactivity. Reaction energies computed for the reactions conducted in water are negative, *i.e.* water drives these reactions to the right.

This work yields quantities that may be inaccessible, or complementary to experiments, and represents the first quantum chemical approach in which both the gas-phase and solvated-phase complexation between charged arginine and lysine molecules and carboxylate, N- and O-sulphate anions modeling heparin–protein interactions are considered, and absolute energies of hydrogen bond pairing interactions were evaluated.

Acknowledgements

This work has been supported by The European Union HPC-Europa Transnational Access Program under the Project HPC-Europa2 (Project No 863) at SARA Amsterdam. The authors acknowledge with thanks the Stichting Academisch Rekencentrum Amsterdam (SARA) for the use of its resources and for excellent support. M. R. thanks the Department of Theoretical Chemistry, Zernike Institute for Advanced Materials, University of Groningen, for its hospitality during his study stay in Groningen.

References

1 U. R. Desai, *Med. Res. Rev.*, 2004, **24**, 151–181.
2 R. J. Linhardt, *J. Med. Chem.*, 2003, **46**, 2551–2564.
3 J. Liu and S. C. Thorp, *Med. Res. Rev.*, 2002, **22**, 1–25.
4 D. L. Rabenstein, *Nat. Prod. Rep.*, 2002, **19**, 312–331.
5 D. A. Lane and U. Lindahl, *Heparin – Chemical and Biological Properties*, CRC Press, Boca Raton, FL, 1989.
6 B. Casu and U. Lindahl, *Adv. Carbohydr. Chem. Biochem.*, 2001, **57**, 159–206.
7 N. S. Gandhi and R. L. Mancera, *Drug Discovery Today*, 2010, **15**, 1058–1069.
8 I. Capila and R. J. Linhardt, *Angew. Chem., Int. Ed.*, 2002, **41**, 390–412.
9 J. M. Walenga, M. Petitou, M. Samama, J. Fareed and J. Choay, *Thromb. Res.*, 1988, **52**, 553–563.
10 M. Petitou and C. A. A. van Boeckel, *Angew. Chem., Int. Ed.*, 2004, **43**, 3118–3133.
11 L. Jin, J. P. Abrahams, R. Skinner, M. Petitou, R. N. Pike and R. W. Carrell, *Proc. Natl. Acad. Sci. U. S. A.*, 1997, **94**, 14683–14688.
12 C. A. A. van Boeckel, P. D. J. Grootenhuis and A. Visser, *Nat. Struct. Biol.*, 1994, **1**, 423–425.
13 C. Noti and P. H. Seeberger, *Chem. Biol.*, 2005, **12**, 731–556.
14 L. Huang and R. J. Kerns, *Bioorg. Med. Chem.*, 2006, **14**, 2300–2313.
15 D. P. Mascotti and T. M. Lohman, *Biochemistry*, 1995, **34**, 2908–2915.
16 J. R. Fromm, R. E. Hileman, E. E. O. Caldwell, J. M. Weiler and R. J. Linhardt, *Arch. Biochem. Biophys.*, 1995, **323**, 279–287.
17 R. E. Hileman, J. R. Fromm, J. M. Weiler and R. J. Linhardt, *BioEssays*, 1998, **20**, 156–167.
18 A. Ori, P. Free, J. Courty, M. C. Wilkinson and D. G. Fernig, *Mol. Cell. Proteomics*, 2009, **8**, 2256–2265.
19 B. S. Blaum, J. A. Deakin, C. M. Johansson, A. P. Herbert, P. N. Barlow, M. Lyon and D. Uhrin, *J. Am. Chem. Soc.*, 2011, **132**, 6374–6381.
20 L. Jin, J. P. Abrahams, R. Skinner, M. Petitou, R. N. Pike and R. W. Carrell, *Proc. Natl. Acad. Sci. U. S. A.*, 1997, **94**, 14683–14688.
21 W. Li, J. D. Johnson, Ch. T. Esmon and J. A. Huntington, *Nat. Struct. Mol. Biol.*, 2004, **11**, 857–862.
22 J. D. Johnson, W. Li, T. E. Adams and J. A. Huntington, *EMBO J.*, 2006, **25**, 2029–2037.
23 D. R. Coombe and W. C. Kett, *Cell. Mol. Life Sci.*, 2005, **62**, 410–424.
24 A. Imberty, H. Lortat-Jacob and S. Pérez, *Carbohydr. Res.*, 2007, **342**, 430–439.
25 M. J. Frisch, G. W. Trucks, H. B. Schlegel, G. E. Scuseria, M. A. Robb, J. R. Cheeseman, Jr. J. A. Montgomery, T. Vreven, T. K. N. Kudin, J. C. Burant, J. M. Millam, S. S. Iyengar, J. Tomasi, V. Barone, B. Mennucci, M. Cossi, G. Scalmani, N. Rega, G. A. Petersson, H. Nakatsuji, M. Hada, M. Ehara, K. Toyota, R. Fukuda, J. Hasegawa, M. Ishida, T. Nakajima, Y. Honda, O. Kitao, H. Nakai, M. Klene, X. Li, J. E. Knox, H. P. Hratchian, J. B. Cross, C. Adamo, C. Jaramillo, R. Gomperts, R. E. Stratmann, O. Yazyev, A. J. Austin, R. Cammi, C. Pomelli, J. W. Ochterski, P. Y. Ayala, K. Morokuma, G. A. Voth, P. Salvador, J. J. Dannenberg, V. G. Zakrzewski, S. Dapprich, A. D. Daniels, M. C. Strain,

O. Farkas, D. K. Malick, A. D. Rabuck, K. Raghavachari, J. B. Foresman, J. V. Ortiz, Q. Cui, A. G. Baboul, S. Clifford, J. Cioslowski, B. B. Stefanov, G. Liu, A. Liashenko, P. Piskorz, I. Komaromi, R. L. Martin, D. J. Fox, T. Keith, M. A. Al-Laham, C. Y. Peng, A. Nanayakkara, M. Challacombe, P. M. W. Gill, B. Johnson, W. Chen, M. W. Wong, C. Gonzalez and J. A. Pople, Gaussian 03, Version 6.0, Gaussian Inc., Wallingford, CT, 2003.

26 M. J. Frisch, G. W. Trucks, H. B. Schlegel, G. E. Scuseria, M. A. Robb, J. R. Cheeseman, G. Scalmani, V. Barone, B. Mennucci, G. A. Petersson, H. Nakatsuji, M. Caricato, X. Li, H. P. Hratchian, A. F. Izmaylov, J. Bloino, G. Zheng, J. L. Sonnenberg, M. Hada, M. Ehara, K. Toyota, R. Fukuda, J. Hasegawa, M. Ishida, T. Nakajima, Y. Honda, O. Kitao, H. Nakai, T. Vreven, J. A. Montgomery Jr., , J. E. Peralta, F. Ogliaro, M. Bearpark, J. J. Heyd, E. Brothers, K. N. Kudin, V. N. Staroverov, R. Kobayashi, J. Normand, K. Raghavachari, A. Rendell, J. C. Burant, S. S. Iyengar, J. Tomasi, M. Cossi, N. Rega, J. M. Millam, M. Klene, J. E. Knox, J. B. Cross, V. Bakken, C. Adamo, J. Jaramillo, R. Gomperts, R. E. Stratmann, O. Yazyev, A. J. Austin, R. Cammi, C. Pomelli, J. W. Ochterski, R. L. Martin, K. Morokuma, V. G. Zakrzewski, G. A. Voth, P. Salvador, J. J. Dannenberg, S. Dapprich, A. D. Daniels, Ö. Farkas, J. B. Foresman, J. V. Ortiz, J. Cioslowski and D. J. Fox, Gaussian 09, Version 9.0, Gaussian Inc., Wallingford, CT, 2011.

27 R. G. Parr and W. Wang, *Density-Functional Theory of Atoms and Molecules*, Oxford University Press, New York, 1994.

28 R. Neumann, R. H. Nobes and N. C. Handy, *Mol. Phys.*, 1996, **87**, 1–36.

29 F. M. Bickelhaupt and E. J. Baerends, in *Rev. Comput. Chem.*, ed. K. B. Lipkowitz, D. B. Boyd, Wiley-VCH, New York, 2000, 15, pp 1–86.

30 A. D. Becke, *Phys. Rev.*, 1988, **A38**, 3098–3100.

31 A. D. Becke, *J. Chem. Phys.*, 1993, **98**, 5648–5652.

32 C. Lee, W. Yang and R. G. Parr, *Phys. Rev.*, 1988, **B37**, 785–789.

33 S. Grimme, *J. Comput. Chem.*, 2006, **27**, 1787–1799.

34 J. E. Del Bene, *Int. J. Quantum Chem.*, 1992, **26**, 527.

35 J. E. Del Bene, *Struct. Chem.*, 1989, **1**, 19–27.

36 A. T. Pudzianowski, *J. Chem. Phys.*, 1995, **102**, 8029–8039.

37 J. Granatier, M. Pitoňak and P. Hobza, *J. Chem. Theory Comput.*, 2012, **8**, 2282–2292.

38 S. F. Boys and F. Bernardi, *Mol. Phys.*, 1970, **19**, 553–566.

39 M. Remko and B. M. Rode, *J. Phys. Chem. A*, 2006, **110**, 1960–1967.

40 M. Remko and C. W. Von der Lieth, *J. Chem. Inf. Model.*, 2006, **46**, 1194–1200.

41 S. Miertuš, E. Scrocco and J. Tomasi, *Chem. Phys.*, 1981, **55**, 117–129.

42 A. Klamt and G. Schűűman, *J. Chem. Soc., Perkin Trans. 2*, 1993, 799–805.

43 V. Barone and M. Cossi, *J. Phys. Chem. A*, 1998, **102**, 1995–2001.

44 M. Cossi, N. Rega, G. Scalmani and V. Barone, *J. Comput. Chem.*, 2003, **24**, 669–681.

45 A. Loß, P. Bunsmann, A. Bohne, A. Loß, E. Schwarzer, E. Lang and C. W. von der Lieth, *Nucleic Acids Res.*, 2002, **30**, 405–408.

46 A. Bohne, E. Lang and C. W. von der Lieth, *Bioinformatics*, 1999, **15**, 767–768.

47 T. Lütteke, M. Frank and C. W. von der Lieth, *Carbohydr. Res.*, 2004, **339**, 1015–1020.

48 T. Lütteke, M. Frank and C. W. von der Lieth, *Nucleic Acids Res.*, 2005, **33**. Database Issue: D242-246.

49 M. Remko, M. Swart and F. M. Bickelhaupt, *J. Phys. Chem. B*, 2007, **111**, 2313–2321.

50 V. S. R. Rao, P. K. Qasba, P. V. Balaji and R. Chandrasekaran, *Conformation of Carbohydrates*. Harwood Academic Publishers, Amsterdam, 1998, p. 56.

51 http://research.chem.psu.edu/brpgroup/pKa_compilation.pdf.

52 S. Hilal, S. W. Karickhoff and L. A. Carreira, *Quant. Struct.–Act. Relat.*, 1995, **14**, 348–355.

53 S. Hilal, S. W. Karickhoff and L. A. Carreira, *QSAR Comb. Sci.*, 2003, **22**, 565–574.

54 J. Tomasi, B. Mennucci and R. Cammi, *Chem. Rev.*, 2005, **105**, 2999–3094.

55 J. Kongsted, P. Söderhjelm and U. Ryde, *J. Comput.-Aided Mol. Des.*, 2009, **23**, 395–409.

56 J. L. Del Bene, *J. Comput. Chem.*, 1989, **10**, 603–615.

57 H. Kubinyi, Hydrogen Bonding: The Last Mystery in Drug Design? in *Pharmacokinetic optimization in drug research: biological, physicochemical, and computational strategies*,ed. B. Testa, H. van de Waterbeemd, G. Folkers, R. Guy, Helvetica Chimica Acta, Zürich, Switzerland, 1st edn, 2001, pp 513–524.

58 M. Nocker, S. Handschuh, Ch. Tautermann and K. R. Liedl, *J. Chem. Inf. Model.*, 2009, **49**, 2067–2076.

59 C. M. Dreef-Tromp, J. E. M. Basten and C. A. A. van Boeckel, Structure activity relationships of synthetic heparin-like oligosaccharides in *Medicinal Chemistry into the Millennium (Special Publication)*, ed. M. M. Campbell and I. A. Blagborough, RSC, Cambridge, 1999.

60 M. Remko, P. T. Van Duijnen and C. W. von der Lieth, *THEOCHEM*, 2007, **814**, 119–125.

61 J. Burgess, *Metal Ions in Solution*. Chichester, Elles Horwood, 1978, pp. 182 and 187. ISBN 0-85312-027-7.

